Energy Impact of Connected Eco-driving on Electric Vehicles

Xuewei Qi, Matthew J. Barth, Guoyuan Wu, Kanok Boriboonsomsin and Peng Wang

Abstract Transportation-related energy consumption and air quality problems have continued to attract public attentions. A variety of emerging technologies have been proposed and/or developed to address these issues. In recent years, electric vehicles (EVs) are deemed to be very promising in reducing traffic related fuel consumption and pollutant emissions, due to the use of electric batteries as the only energy source. On the other hand, recent research shows that additional energy savings can be achieved with the aid of Eco-driving system in a connected vehicle environment (e.g., Eco-approach at signalized intersections). However, most of the existing eco-driving research is only focused on the internal combustion engine (ICE) vehicles thus far. There is still lack of convincing evidence (especially with real-world implementation) of how these connected eco-driving technologies impacts the energy efficiency of EVs. To fill this gap, this chapter provides a real-world example of quantifying the energy synergy of combining vehicle connectivity, vehicle automation and vehicle electrification, by designing, implementing and testing an eco-approach and departure (EAD) system for EVs with real-world driving data.

Keywords Electric vehicles · Eco-driving · Vehicle automation · Connected vehicle · Energy impact · Traffic signals

X. Qi (✉) · M.J. Barth · G. Wu · K. Boriboonsomsin · P. Wang
Department of Electrical and Computer Engineering, University of California-Riverside, Riverside, CA 92521, USA
e-mail: xqi001@ucr.edu

M.J. Barth
e-mail: barth@ee.ucr.edu

G. Wu
e-mail: gywu@cert.ucr.edu

K. Boriboonsomsin
e-mail: kanok@cert.ucr.edu

P. Wang
e-mail: pewang@engr.ucr.edu

G. Meyer and S. Beiker (eds.), *Road Vehicle Automation 4*,
Lecture Notes in Mobility, DOI 10.1007/978-3-319-60934-8_10

1 Introduction

In recent years, a significant amount of transportation-related fossil fuel consumption and greenhouse gas emissions have created an increasing amount of public concern. Tailpipe emissions from vehicles are the single largest human-made source of carbon dioxide, nitrogen oxides, and methane in transportation related activities. Vehicles that are stationary, idling, and traveling in a stop-and-go pattern due to congestion in urban areas emit more pollutant emissions and greenhouse gases (GHGs) than those traveling in free-flow conditions. The resulted air quality degradation is very serious in some major cities of U.S. as well as other developing countries (e.g., China).

In addition to improving air quality, reducing transportation-related energy consumption and greenhouse gas (GHG) emissions has been a common goal of public agencies and research institutes for many years. In 2014, the total energy consumed by the transportation sector in the United States was as high as 23.70 Quadrillion BTU which is 28% share of the total energy (U.S. Energy Information Administration 2015) (see Figs. 1 and 2). The U.S. Environmental Protection Agency (EPA) reported that nearly 26% of GHG emissions resulted from fossil fuel combustion for transportation activities in 2014 (U.S. Environmental Protection Agency (EPA) 1990) (see Fig. 1a, b).

Altogether, the transportation-related impacts on air quality, climate change, and energy consumption have motivated researchers from different technical backgrounds to develop different ways to reduce vehicle emissions and energy consumption. In recent years, with the rapid development of vehicle related technologies, such as connected vehicle (CV) technology as well as automation technology, there is now a common vision for future vehicles that will be

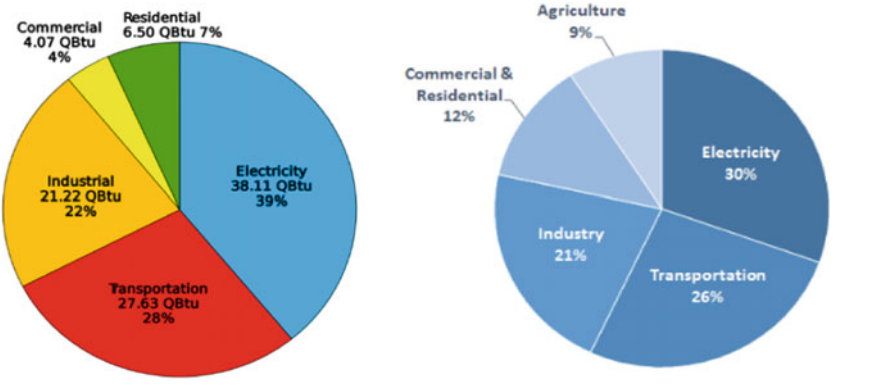

a) Energy Consumption 2014 [1] b) Total U.S. Greenhouse Gas Emissions 2014 [2]

Fig. 1 Total U.S. energy consumption and greenhouse gas emissions by economic sectors **a** Energy Consumption 2014 (U.S. Energy Information Administration 2015). **b** Total U.S. greenhouse gas emissions 2014 (U.S. Environmental Protection Agency (EPA) 1990)

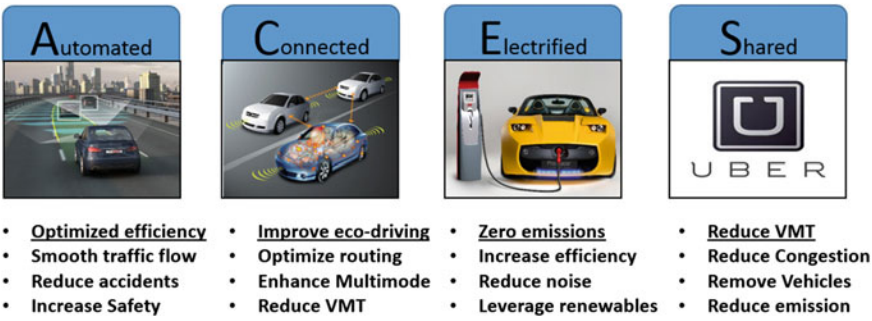

Fig. 2 Key features of future vehicles

automated, connected, electrified and shared. As can be seen in Fig. 2, for each of those features, multiple benefits can be identified (as listed in the figure) in terms of safety, mobility and environmental impact. However, reducing energy consumption and emissions are the only benefits that can be achieved in all four of these features. This is explained in more detail below:

1. **Automated**: Vehicle automation including automated vehicle dynamics control (i.e., adaptive cruise control (ACC)) and automated powertrain operations (i.e., power-split control for PHEVs), can be used to improve vehicle energy efficiency and reduce emissions. For example, eco-friendly adaptive cruise control (Eco-ACC) is designed to automatically control the vehicle speed profile when following a preceding vehicle smoothly to reduce unnecessary accelerations so that energy efficiency can be improved.
2. **Connected**: The recent development of Connected vehicle (CV) technology has brought a new revolution for the modern intelligent transportation system. In a CV environment, the V2V, V2I communications enables unlimited potential applications. For example, connected ecodriving technology is designed in a CV environment to encourage more energy efficient driving, such as reducing traffic congestion and unnecessary stop-and-go maneuvers at signalized intersections.
3. **Electrified**: In recent years, cleaner alternative energy sources are used to replace fossil fuels for vehicles, such as electricity from renewable resources (e.g., solar, wind) and hydrogen. With these alternative fuels, plug-in electric vehicles (PEVs) and fuel cell vehicles are designed. Transportation electrification is one of the more promising ways to reduce transportation related fossil fuel consumption and emissions; however, the massive adoption of PEVs is currently impeded by the limited charging infrastructure and the perceived limited driving range per charge (i.e., the so-called "range anxiety") (Zhang and Yao 2015). There is still large room for improving PEV energy efficiency.
4. **Shared**: Vehicle Systems have emerged in the last two decades provide a variety of shared mobility options. Shared vehicle systems have had this tremendous growth due to advances in electronic and wireless technologies that

made sharing assets easier and more efficient. The main benefits of shared vehicle systems is to reduce vehicle miles travelled (VMT), thereby reducing vehicle energy consumption and tailpipe emissions.

As previously described, the adoption of electric-drive vehicles has the potential to play a significant role in addressing both energy and environmental impacts brought by on by today's transportation systems. Using electricity as a transportation fuel has a number of benefits. Electricity has a strong potential for GHG reduction, as long as it is generated from renewable sources such as solar and wind. Electric vehicles themselves have zero direct emissions, although generating the electricity to power the vehicle often results in indirect emissions at the power plants. If electricity is generated from the current U.S. average generation mix, EVs can reduce GHG emissions by about 33%, compared to today's ICE powered vehicles (US DOT 2010). If we assume 56% light-duty vehicle (LDV) penetration by 2050, this could provide a total reduction in transportation emissions of 26–30% (US DOT 2010). The huge potential benefits of EVs have already attracted significant interest and investment in EV technology. Since late 2010, more than 20 automakers have introduced BEVs or PHEVs. Within the United States, the government has allocated considerable stimulus funding to promote the use of alternative fuels (Skerlos and Winebrake 2010). The American Recovery and Reinvestment Act (ARRA) of 2009 provided over $2 billion for electric vehicle and battery technologies, geared toward achieving a goal of one million electric vehicles on U.S. roads by 2018 (Canis 2011). Many states also have committed themselves to promoting EVs. For example, California has taken a number of legislative and regulatory steps to promote electric vehicle deployment and adoption, such as the Zero Emission Vehicle and Low Carbon Fuel Standard regulatory programs and rebates for purchasing electric vehicles (Elkind 2012). With this momentum, it is not difficult to see that in the near future EVs may gain significant market penetration, particularly in densely populated urban areas with systemic air quality problems.

This chapter is aimed at investigating the synergy energy benefits of vehicle electrification, vehicle automaton and vehicle connectivity by designing, implementing and testing a connected ecodriving technology for EVs. Researchers have proposed several eco-driving systems that are capable of optimizing EV energy efficiency under different driving conditions. An eco-friendly optimal adaptive cruise control (ACC) was developed in (Flehmig et al. 2015). It calculates an energy optimal trajectory for an EV when following another slower vehicle in traffic. (Frank e al. 2013) designed an Android application to inform the driver about the energy efficiency by calculating and showing an eco-score based on a fuzzy system. A novel torque vectoring control system that can optimally distribute the torque by considering the efficiency characteristics of EVs was proposed in (Koehler et al. 2015) and 10% of energy efficiency improvement was identified. Despite the above efforts on eco-driving systems for EVs, only a few are focused on the eco-approach and departure (EAD) system which takes advantage of signal phase and timing (SPaT) information broadcast via infrastructure-to-vehicle

(I2V) communication. (Miyatake et al. 2011) applied a dynamic programming (DP)-based model to develop eco-driving systems for EVs along signalized arterials. The proposed model was tested in simulation with very limited signal phase conditions. In a recent study (Zhang and Yao 2015), the authors developed an EAD system for EVs based on their own EV energy consumption estimation model, where the validation was also conducted in a simulation environment under 4 scenarios with different signal phases. In this chapter, an EAD system for EVs was developed and evaluated in two different automation levels: manual driving with assistance via human-machine interface (HMI) and partially automated longitudinal control. Real-world driving data were collected for system evaluation, by comparing the energy and mobility performance to the baseline stage, i.e., manual driving without any assistance.

2 Connected Eco-driving for EV

2.1 Vehicular Movements at Isolated Intersections

Basically, there are 4 different *passing scenarios* for a vehicle to travel through an isolated signalized intersection. The velocity profiles of these 4 different scenarios are shown by the green, blue, red, and yellow lines in Fig. 3. It is also noted that all these trajectories have the same initial and final velocities, and same traveled distance (e.g., within the dedicated short range communication range). More specifically, these scenarios can be described as follows:

- Scenario 1 (cruise): the vehicle cruises through the intersection at a constant speed (green line)

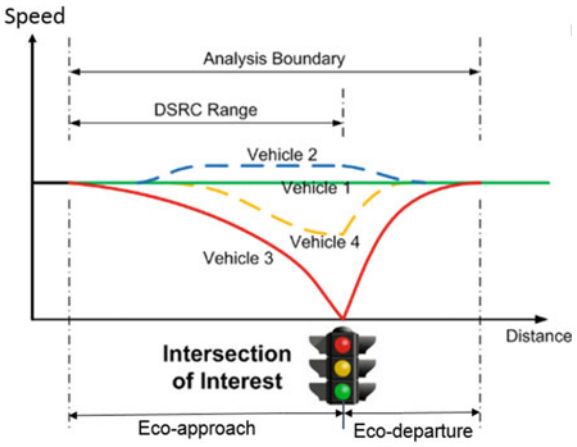

Fig. 3 Illustration of different vehicle trajectories traveling across an intersection

- Scenario 2 (speed-up): the vehicle speeds up to pass the intersection and then gets back to the initial speed after the intersection (blue line)
- Scenario 3 (coast-down with stop): the vehicle slows down and stops at the intersection (red line)
- Scenario 4 (coast-down without stop or glide): the vehicle slows down and passes the intersection at a mid-range speed, and then speeds up to its initial speed (yellow line)

For conventional gasoline vehicles, our previous research (Barth et al. 2011) has shown that, even though all these scenarios cover the same distance with the identical initial and final velocities, the associated fuel consumption and emissions may vary greatly. Vehicle 1 (or Scenario 1) uses the least fuel since it does not need to accelerate or make unnecessary deceleration. Vehicle 2 (or Scenario 2) consumes more fuel than vehicle 1 since there is a slight acceleration and deceleration before and after the intersection. Vehicle 3 (or Scenario 3) might use the most amount of fuel since it has to decelerate to a full stop, idle for a certain period, and then accelerate from a stop to a desired final speed. Finally, Vehicle 4's (or Scenario 4's) fuel consumption may be comparable to Vehicle 2's since both vehicles have a slight speed up and slow down during their trips, although the acceleration occurs at a relatively lower speed.

Therefore, when a gasoline vehicle is traveling through a signalized intersection, its velocity profile could be optimized to achieve minimum fuel consumption for each of the 4 scenarios. Similarly, the velocity profile of an EV can also be optimized to achieve minimum energy consumption by taking into consideration of its distinctive characteristics (e.g., regenerative braking). This is the basic idea behind the vehicle trajectory planning algorithm described in the following.

2.2 Optimal Vehicle Trajectory Planning

In this study, a vehicle trajectory planning algorithm (VTPA) is designed for generating an optimal velocity profile based on real-time SPaT information. Among all the possible velocity profiles with which a vehicle can safely travel through an intersection, the VTPA can choose the velocity profile that has minimum tractive power requirements, in order to minimize energy consumption. The required tractive power of a vehicle depends on the instantaneous velocity and acceleration under the point mass assumption, as given by:

$$P_{tract.} = Av + Bv^2 + Cv^3 + M(0.447a + g\ \sin\theta)v * 0.4471000 \qquad (1)$$

where M is vehicle mass with appropriate inertial correction for rotating and reciprocating parts (kg); v is instantaneous speed (miles/hour or mph); a is acceleration (mph/s); g is gravitational acceleration (9.81 meters/second^2 or m/s^2); and θ is road grade angle in degree. Here, the coefficients A, B, and C are associated with

rolling resistance, speed-correction to rolling resistance, and aerodynamic drag, respectively, which can be determined empirically.

As suggested in our previous work (U.S. Energy Information Administration 2015), there are numerous ways to accelerate or decelerate from one speed to another, such as constant acceleration and deceleration rates, linear acceleration and deceleration rates, and constant power rates. A family of piecewise trigonometric-linear functions is selected as the target velocity profiles (for both approach and departure portions), due to its mathematical tractability and smoothness. For more details of the algorithm, please refer to (U.S. Energy Information Administration 2015).

2.3 *MPC-Based EAD System for Partially Automated Driving*

In this study, the designed VTPA is integrated with a model predictive control (MPC) scheme to develop a partially automated EAD system for EVs (see Fig. 4). For each optimization time horizon of the proposed system, the control objective is to follow the pre-calculated optimal vehicle trajectory as close as possible. In addition, the receding horizon property of MPC allows the system to better handle unpredicted disturbances. The system diagram is provided in Fig. 4.

A nonlinear point mass model (longitudinal dynamics) (Kamal et al. 2013) is adopted in this work:

$$\dot{x} = v, \tag{2a}$$

$$\dot{v} = -\frac{1}{M} C_D \rho_a A_v v^2 - \mu g - g\theta + u_f, \tag{2b}$$

where x is position of the vehicle; v is velocity; M is mass; θ is road gradient ($\theta = 0$ in this work); g is acceleration of gravity (i.e., 9.8 m/s^2); u_f is braking or traction force per unit mass (i.e., the acceleration/deceleration generated from vehicle propulsion); C_D is drag coefficient; ρ_a is air density; A_v is frontal area of the

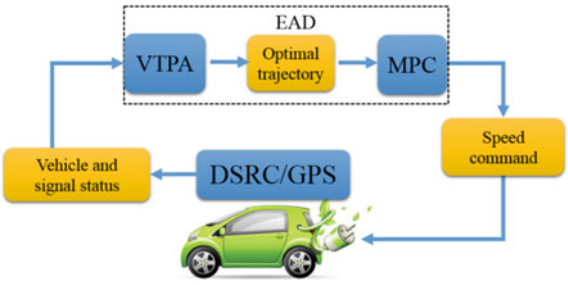

Fig. 4 The system diagram of MPC-based EAD for EVs

vehicle; and μ is rolling friction coefficient. The values of C_D, ρ_a, A_v, and μ can be found in (Kamal et al. 2013). When implementing MPC, Eq. (2a) needs to be discretized as follows:

$$x(t_0 + (k+1)\Delta t) = x(t_0 + k\Delta t) + v(t_0 + k\Delta t)\Delta t, \tag{3a}$$

$$\begin{aligned} v(t_0 + (k+1)\Delta t) = v(t_0 + k\Delta t) \\ + (-\frac{1}{M} C_D \rho_a A_v v(t_0 + k\Delta t)^2 \\ - \mu g - g\theta + u_f(t_0 + k\Delta t))\Delta t, \end{aligned} \tag{3b}$$

where t_0 is starting time, Δt is sampling period, and k is time step. For brevity, we denote $x(t_0 + k\Delta t)$ as $x(k)$, $v(t_0 + k\Delta t)$ as $v(k)$, and $u_f(t_0 + k\Delta t)$ as $u_f(k)$ in the remaining parts of this work.

As stated above, the MPC is designed to follow the optimal vehicle trajectory. Therefore, the objective function is defined as the sum of squared differences between the modeled and reference velocities. We also consider box constraints for the velocities, acceleration/deceleration and jerk values. In summary, the optimal control problem based on MPC can be formulated as:

$$\begin{aligned} \text{argmin}_{u_f} \quad & \sum_{k=t}^{t+l} [v(k) - v_r(k)]^2, \\ \text{subject to} \quad & \text{the discritized dynamics } (3), \\ & v_m \le v(k) \le v_M, \\ & \left|u_f(k)\right| \le u_M, \\ & \left|u_f(k+1) - u_f(k)\right| \le du_M, \end{aligned}$$

where t is current time; l is optimization horizon; $v(\cdot)$ is velocity computed by the MPC; $v_r(\cdot)$ is reference velocity; v_m is minimum allowable speed, which is set to 0 in this work; v_M is maximum allowable speed (usually the speed limit); u_M is maximum acceleration/deceleration constrained by the vehicle propulsion power; and du_M is the user-defined maximum jerk (mainly for driving comfort). We use 0.1 s as the time step and the control horizon of the MPC is set to 1 s, which means that there are 10 time steps to optimize for each control horizon. Note that as the dynamics in Eq. (3a) are nonlinear, the optimization problem at every time step of the MPC is non-convex.

3 Experimental Design and Data Collection

The field data for evaluation were collected at the Turner-Fairbank Highway Research Center (TFHRC) in McLean, Virginia. The driving test was conducted from point "*A*" to point "*B*" with a length of 190 ft before the intersection and 126 ft

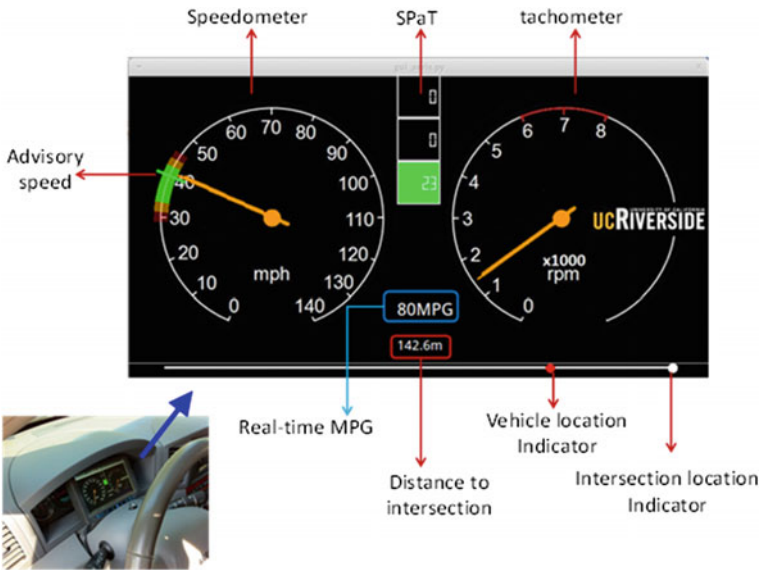

Fig. 5 Graphic interface for "manual-HMI-assisted" driving

after the intersection (see Fig. 5). In order to comprehensively investigate the energy and mobility benefits of the proposed system for EVs, we evaluated the system performance in 3 different stages as elaborated in the following:

- Stage I: "manual-uninformed" driving (MUD) as a baseline. In this stage, the driver approached and traveled through the intersection in a normal fashion without guidance or automation, stopping as needed without any guidance or automated vehicle control.
- Stage II: "manual-HMI-assisted" driving (HMI). In this stage, the driver was provided an enhanced dashboard which presented a recommended range of driving speed overlaid on a speedometer (see Fig. 5). This information can assist the driver to approach and depart the intersection in an environmentally friendly manner while obeying the traffic signal. The advisory speed profiles were generated using the VTPA described earlier.
- Stage III: "MPC-based (partially) automated" driving (MPC). No real-world testing has been conducted in this stage due to the limited resources. Instead, we evaluated the performance of the designed MPC-based longitudinal control system in a simulation environment developed in Matlab using data collected from the field testing. The optimal speed profile calculated by the VTPA was used as the reference input to the MPC model. The results from this simulation likely represent the upper bound of system performance.

To investigate different scenarios with respect to when a vehicle enters a signalized intersection, the field experiment was designed to have the test vehicle

approach the intersection at different time instances throughout the entire signal cycle (i.e., every 5 s in the 60-s cycle). We call these different entering cases as "*entry case*" in the rest of this chapter. Furthermore, the test vehicle approached the intersection at different operating speeds (i.e., 20 and 25 mph). Therefore, a test matrix was designed, consisting of the operating speed along the vertical axis, and the *entry case* across the horizontal access. In this matrix, there are a total of 12 *entry cases* × 2 speed levels = 24 test cells. For the Stage I and Stage II experiments, a total of four drivers were recruited to conduct test runs. Each driver completed each of the test cells in the test matrix. Therefore, a total of 24 test cells × 2 stages × 4 drivers = 192 test runs were conducted. For each test run, data such as speed and distance to the stop bar were logged at 10 Hz and post-processed to determine energy consumption and other performance measures. It is noted that a hybrid vehicle (2012 Ford Escape) was used for the field study. The energy consumption was estimated by the EV energy consumption model (see Sect. 4) under the assumption that there would be no significant change in driving speed if an EV were used.

4 Energy and Mobility Benefits Analysis

4.1 EV Energy Consumption Estimation Model

A microscopic EV energy consumption estimation model developed in (Zhang and Yao 2015) was adopted to calculate the EV energy consumption based on the collected vehicle speed profiles. This model is designed for 4 different EV driving conditions: accelerating, decelerating, cruising and idling. The final model is presented as follows:

$$ECR = \begin{cases} e^{(\sum_{i=0}^{3}\sum_{j=0}^{3}(l_{i,j}\times v^i\times a^j))} & a>0 \\ e^{(\sum_{i=0}^{3}\sum_{j=0}^{3}(m_{i,j}\times v^i\times a^j))} & a<0 \\ e^{(\sum_{i=0}^{3}(n_i\times v^j))} & a=0, v\neq 0 \\ \overline{const} & a=0, v=0 \end{cases} \tag{4}$$

where, *ECR* is energy consumption rate (Watt); $l_{i,j}, m_{i,j,}$ and n_i are coefficients for ECR at speed power index i (=0, 1, 2, 3) and acceleration power index j (=0, 1, 2, 3); v is instantaneous speed (km/h); a is instantaneous acceleration (m/s^2); $\overline{const}$ is the average energy consumption rate for idling. The coefficients in this model were obtained through curve fitting of real-world driving data and can be found in (Zhang and Yao 2015).

4.2 Energy and Mobility Benefits Analysis

Using the data collected in the field test, the designed EAD system for EVs were evaluated in terms of energy and motility benefits. The EV energy consumption model described above was applied to calculate the energy consumption associated with the collected vehicle trajectory data. Figure 6 indicates the change in *passing scenarios* due to the application of the EAD system for one of the drivers (Driver 1). For example, in *entry case* 4, Driver 1 passed the intersection with passing scenario 3 (which is the most energy intensive passing scenario) in both stages I and II, but he would have done so with passing scenario 2 in stage III if the proposed MPC-based longitudinal controller has been applied. It is observed that among the 12 *entry cases* of Driver 1, there are more scenario 3 in stage I than that in stage II or stage III due to the lack of recommended driving speed provided to the driver. In stage III, there would have been no passing scenario 3 with the aid of the MPC-based longitudinal controller.

Figure 7a, b show the energy savings and time savings of stage II ("HMI vs. MUD") and stage III ("MPC vs. MUD"), as compared to stage I, for Driver 1. Figure 6 shows clearly that most of the energy savings happen when the *passing scenarios* changes from scenario 3 to scenario 2 or scenario 4 (i.e., entry cases 3, 4, 5, 6, and 7 shown in Fig. 6). The biggest energy saving (45.3%) occurs in *entry case* 4 where the *passing scenario* changes from scenario 3 to scenario 2. The speed profiles for this entry case are given in Fig. 8a. As shown in the figure, when given the advisory speed profile through HMI, Driver 1 failed to follow it closely at the beginning, resulting in a switch from passing scenario 2 to 3, and therefore, trivial energy savings. For those *entry case*s where the three different stages are in the

Signal Phase	Entering Time(s)	Entry Case	MUD	HMI	MPC
Green	2	1	1	1	1
	7	2	2	2	2
	12	3	3	3	2
	17	4	3	3	2
	22	5	3	3	4
	27	6	3	3	4
Red	2	7	3	4	4
	7	8	4	4	4
	12	9	1	1	1
	17	10	1	1	1
	22	11	1	1	1
	27	12	1	1	1

Scenario 1 Scenario 2 Scenario 3 Scenario 4

Fig. 6 Changes in passing scenario in different stages (Driver 1)

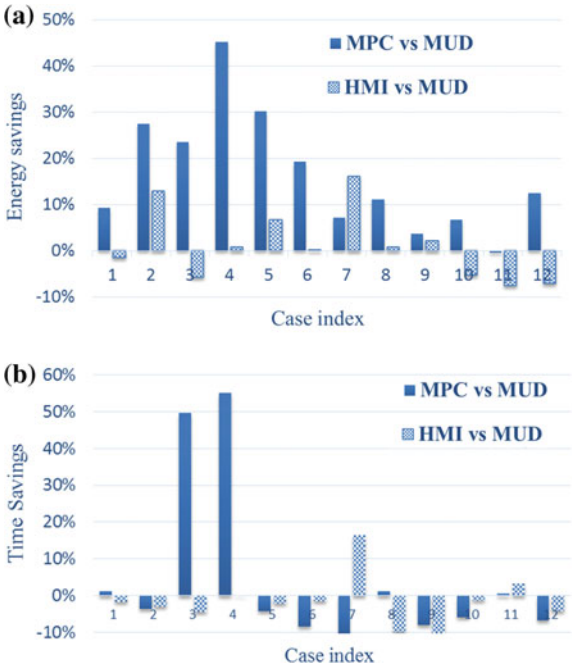

Fig. 7 **a** Energy and time savings for different entry cases (Driver 1)—Energy savings. **b** Energy and time savings for different entry cases (Driver 1)—Time savings

same *passing scenarios*, the energy savings are not as much and, for some entry cases of stage 2, turn negative because of variations in real-world driving.

From the mobility perspective, it is observed in Fig. 7b that most of the *entry case*s in stage II and stage III result in minimal time savings or even small time penalties except *entry case* 3 and *entry case* 4 of stage III where the passing scenario is 2. This can be well explained by Fig. 8b where the speed profile in stage I shows a more aggressive trend (i.e., exceeding the speed limit of 20 mph almost throughout) than either of the other two stages. Although stages II and III have longer travel times in this case, it is because of the uncharacteristic driving in stage 1 rather than the shortcoming of the EAD system.

To further analyze the energy benefits of the designed EAD system, a scenario change analysis was conducted using the driving data of all 4 drivers. The analysis covers all the scenario changes that happened in the field experiment. As shown in Table 1, most of the energy savings happen when the passing scenario changes from scenario 3 to scenario 2 or scenario 4 with the assistance of the EAD system. However, when the EAD system cannot change the passing scenario, there is not as much energy saving (on average) or even a negative saving (for scenario 3 between stage I and stage II) due to variations in real-world driving. This may suggest that the information disseminated by the HMI is not effective enough in assisting the manual driving and more comprehensive system design should be conducted to take into consideration the human factors aspect. One possible way to improve the

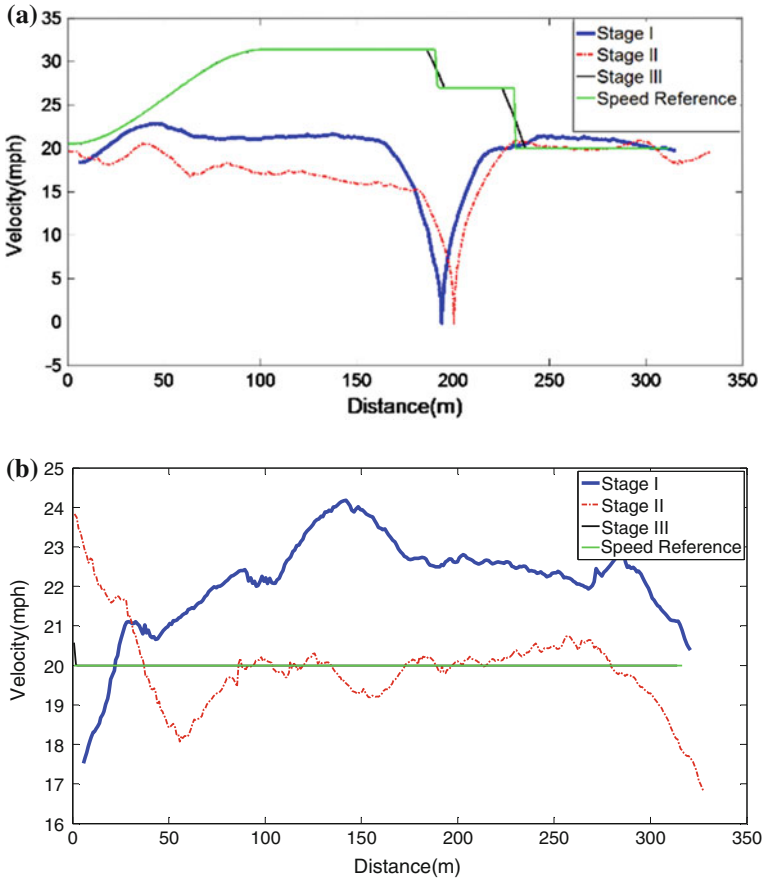

Fig. 8 **a** Speed versus distance for entry case 4 (Driver 1). **b** Speed versus distance for entry case 9 (Driver 1)

existing system is to disable the display of advisory speed when the system predicts that there will be no change in the passing scenario.

Finally, the average energy and time savings across all *entry case*s and all drivers were calculated and thus are provided in Table 2. It shows that the MPC based EAD system can achieve an average of 21.9% electricity savings along with an average of 10.7% time savings (mostly contributed by *entry case* 3 and *entry case* 4), while the driving assistance system with HMI achieves 12.1% energy savings on average but with compromise of travel time (increase of 3.2%).

Table 1 Scenario-change analysis

Stage	Scenario change	Energy savings		
		Min (%)	Mean (%)	Max (%)
I versus III	3 → 2	13.9	25.7	45.3
I versus III	3 → 4	10.3	19.1	27.0
I versus III	1 → 1	−16.0	7.3	11.3
I versus III	2 → 2	−15.5	5.9	10.9
I versus II	3 → 2	2.2	9.5	18.3
I versus II	3 → 4	1.2	3.8	13.9
I versus II	1 → 1	−6.7	1.1	6.3
I versus II	2 → 2	−15.1	0.9	5.1
I versus II	3 → 3	−10.3	−3.1	7.3

Table 2 Average energy and mobility improvement

Stage	Energy benefit (energy savings)			Mobility benefit (time savings)		
	Min (%)	Mean (%)	Max (%)	Min (%)	Mean (%)	Max (%)
II	−14.3	12.1	27	−13	−3.2	17.6
III	3.7	21.9	45.3	−28.1	10.7	55.1

5 Conclusion

Due to the lack of evidence of how vehicle automation, vehicle connectivity could influence the energy efficiency of EVs, this chapter provides numerical evidence of the energy synergy of combining vehicle connectivity, vehicle automation and vehicle electrification, by designing, implementing and testing an eco-approach and departure (EAD) system for EVs with real-world driving data. In this chapter, connected eco-driving system for EVs is developed and then evaluated in two different stages: driving assistance via HMI and partially automated driving. The analyses show that an average of 12 and 22% energy savings can be achieved in these two stages, respectively, compared to the baseline stage (i.e., manual driving without any assistance). To the best of our knowledge, this is the first research that reports the energy benefits of connected eco-driving system for EVs with real-world driving data at different automation levels. Potential topics for future research include improving the system performance by considering the human factors aspect in the design of the HMI and conducting real-world experiments with actual EVs under a variety of scenarios.

References

Barth M, Mandava S, Boriboonsomsin K, Xia H (2011) Dynamic eco-driving for arterial corridors. IEEE forum on integrated and sustainable transportation system (FISTS), Vienna, pp 182–188

Canis B (2011) Battery manufacturing for hybrid and electric vehicles: policy issues. Congressional research service. http://nepinstitute.org/get/CRS_Reports/CRS_Energy/Energy_Efficiency_and_Conservation/Batteries_for_Hybrid_and_Elec_Vehicles.pdf. Accessed 10 Apr 2013

Elkind EN (2012) Electric drive by '25: how California can catalyze mass adoption of electric vehicles by 2025, Workshop by UCLA Law/Berkeley Law. www.law.berkeley.edu/files/ccelp/Electric_Drive_by_25-2.pdf. Accessed 22 Apr 2013

Flehmig F, Sardari A, Fischer U, Wagner A (2015) Energy optimal adaptive cruise control during following of other vehicles. In: IEEE intelligent vehicles symposium (IV), Seoul, pp 724–729

Frank R, Castignani G, Schmitz R, Engel T (2013) A novel eco-driving application to reduce energy consumption of electric vehicles. In: International conference on connected vehicles and expo (ICCVE), Las Vegas, NV, pp 283–288

Kamal MS, Mukai M, Murata J, Kawabe T (2013) Model predictive control of vehicles on urban roads for improved fuel economy. IEEE Trans Control Syst Technol 21(3):831–841

Koehler S, Viehl A, Bringmann O, Rosenstiel W (2015) Improved energy efficiency and vehicle dynamics for battery electric vehicles through torque vectoring control. In: IEEE intelligent vehicles symposium (IV), Seoul, pp 749–754

Miyatake M, Kuriyama M, Takeda Y (2011) Theoretical study on eco-driving technique for an electric vehicle considering traffic signals. In: IEEE ninth international conference on power electronics and drive systems (PEDS), Singapore, pp 733–738

Skerlos SJ, Winebrake JJ (2010) Targeting plug-in hybrid electric vehicle policies to increase social benefits. Energy Policy 38(2):705–708

US DOT (2010) Transportation's role in reducing U.S. greenhouse gas emissions, synthesis report, vol 1, report to congress, U.S. Department of Transportation

U.S. Energy Information Administration: Monthly Energy Review, Table 2.1, Mar 2015. www.eia.gov/Energyexplained/?page=us_energy_transportation

U.S. Environmental Protection Agency (EPA): inventory of U.S. greenhouse gas emissions and sinks: 1990–2014, Final report, Apr 2016

Zhang R, Yao E (2015) Eco-driving at signalised intersections for electric vehicles. IET Intell Transp Syst 9(5):488–497